JPE 11-3-7

A Five-Phase Induction Motor Speed Control System Excluding Effects of 3rd Current Harmonics Component

Min-Huei Kim†, Nam-Hun Kim*, and Won-Sik Baik**

† Dept. of. Automatic Electrical Engineering, Yeungnam College of Science & Technology, Daegu, Korea
* R&D Center, CnM Inc., Keyngnam, Korea
** R&D Center, LS Mecapion, Daegu, Korea

Abstract

In this paper an effective five-phase induction motor (IM) and its drive methods are proposed. Due to the additional degrees of freedom, the five-phase IM drive presents unique characteristics for enhancing the torque producing capability of the motor. Also the five-phase motor drives possess many other advantages when compared to traditional three-phase motor drives. Some of these advantages include, reducing the amplitude and increasing the frequency of the torque pulsation, reducing the amplitude of the current without increasing the voltage per phase and increasing the reliability. In order to maximize the torque per ampere, the proposed motor has concentrated winding, the produced back electromotive force (EMF) is almost trapezoidal, and the motor is supplied with the combined sinusoidal plus the third harmonic of the currents. For demonstrating the superior performance of the proposed five-phase IM, the motors are also analyzed on the synchronously rotating reference frame. To supply trapezoidal current waveform and to exclude the effect of the 3rd harmonic current, a new control stratagem is proposed. The proposed control method is based on direct torque control (DTC) and rotor flux oriented control (RFOC) of the five-phase IM drives. It is able to reduce the acoustical noise, the torque, the flux, the current, and the speed pulsations during the steady state. The DTC transient merits are preserved, while a better quality steady-state performance is produced in the five phase motor drive for a wide speed range. Experimental results clearly demonstrated a more dynamic steady state performance with the proposed control system.

Key Words: 3rd harmonic, DTC, Five-phase motor, IM, RFOC

I. Introduction

In recent years, multi-phase IM, five phase, six phase, seven phase motors and so on, have attracted many researchers and are gaining interest as viable alternative solutions to a three-phase IM system for hybrid electrical vehicle, aircraft and ship propulsion applications [1]-[3].

Some inverters produce rectangular current or voltage pulses rather than sinusoidal so that they are useful in designing new types of machines with concentrated winding distributions which are more compatible with the nature of the supply. If a machine has concentrated windings then the air gap flux could have a rectangular rather than a sinusoidal shape. In machines with sinusoidal air gap flux distributions only a small part of the iron is near saturation. As a result, the iron can be used more effectively, if the air gap flux density has a rectangular form [4]-[9].

Manuscript received Nov. 17, 2010; revised Feb. 28, 2011
Recommended for publication by Associate Editor Kyeong-Hwa Kim.
† Corresponding Author: mhkim@ync.ac.kr
Tel: +82-53-650-9263, Fax: +82-53-624-4736, Yeungnam College of Sci. & Tech.
* R&D Center, CnM Inc., Korea
** R&D Center, LS Mecapion, Korea

A Five-phase motor drive possess many advantages when compared to conventional three-phase IM drives, such as reducing the amplitude and increasing the frequency of the torque pulsation, reducing the rotor harmonic currents, reducing the current per phase without increasing the voltage per phase, lowering the dc link current harmonics, providing higher power density, outputting more torque, and having higher reliability [10], [11].

Higher torque density in a multi-phase machine is possible, since apart from the fundamental spatial field harmonic, the space harmonic fields can be used to contribute to the total torque production. In a multi-phase machine, with five or more phases, there are additional degrees of freedom, which can be used to enhance the torque production through the injection of higher-order current harmonics. In a five-phase induction machine a third harmonic current injection can be used to enhance the overall torque production [5], [12]. In [8], [9], Toliyat et al. also mentioned that most multiphase motors are designed to have a nonsinusoidal back EMF voltage in order to increase the torque per ampere. However, five-phase motors have additional third space harmonics. This space harmonic will result in a considerable harmonic current and cause deformation of the phase current. In order to solve this problem, [15] proposed DTC using space vector modulation (SVM).

The used five-phase IM has two significant differences in the terms of its structure and input current profiles. First, concentrated windings instead of sinusoidal winding are adapted. Second, a trapezoidal current component is introduced into the motor currents. The DTC of an IM is a powerful control method for motor drives. Using DTC instead of field oriented control (FOC) provides good dynamic characteristics and simple implementation [15]. However from the maintenance and reliability perspective, the implementation of DTC is shown to cause bearing currents which result in pitting and fluting of the motor bearings, thereby reducing the life of the motor [6].

The FOC of a five-phase machine with concentrated winding on the stator with current control in the rotating reference frame has been reported [6], [13], [14].

Space vector pulse width modulation (SVPWM) is used to control a five-phase voltage source inverter feeding a drive. Only the outer large vectors are used to realize the SVPWM. However, this method has a complicated control structure and produces unwanted low order harmonics [12], [13].

Considering the above mentioned points, a five phase IM with a concentrated winding and an almost rectangular waveform back EMF, is designed. In order to inject a trapezoidal current waveform and achieve better dynamic performance, a new control method is proposed. The proposed control method is based on RFOC and DTC of five-phase IM drives.

In order to exclude effect of the 3rd harmonic current the RFOC method is adapted during the steady state, and to maintain dynamic characteristics the DTC method is applied during the dynamic state.

In order to implement the proposed control methods, a TMS320F2812 DSP is adopted as the central processor. Experimental results show the excellent performance of this system.

II. Harmonic Analysis And Mathematical Model of A Five-Phase IM

A. Harmonic Analysis

In this section, the following assumptions are made:

- The IM is considered to be operating under steady state conditions.
- Saturation effects are neglected to allow for the superposition of magnetic fields.
- Skin effects in the stator at the harmonic frequency are neglected.

Consider the stator of a machine with an elementary two-pole, five-phase IM with concentrated windings of the N turns, which are 72[deg] apart in space and presented in Fig. 1. The axis of phase "a" is used as a reference point for the circumference angle φ to define the winding function $N(\varphi)$ as shown in Fig. 2, where N is the number of turns per pole in every phase. The winding function waveforms of the phases "b", "c", "d" and "e" can be obtained by shifting 72[deg] from phase "a" according to the order.

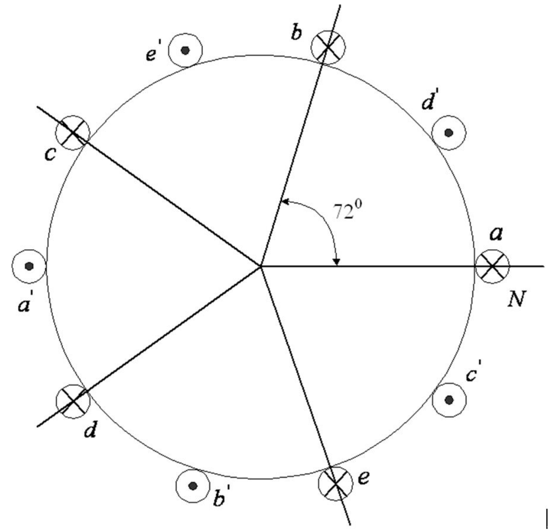

Fig. 1. Five-phase concentrated winding of IM.

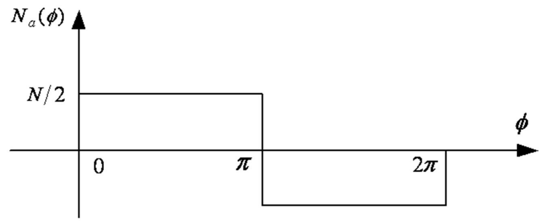

Fig. 2. Winding function for phase "a" of five-phase IM.

The Fourier series of each winding shown in Fig. 2 is follow by eq. (1).

$$N(\phi) = \sum_{n=1}^{\infty} \left(\frac{4}{n\pi}\right) \frac{N}{2} \sin\frac{n\pi}{2} \cos n(\phi + \alpha) \quad n = 1,3,5,\ldots \tag{1}$$

where, ϕ is the spatial angle, α is the spatial angle between the phases (72°), and n is the harmonic order.

Since the winding function is symmetric, the even harmonics do not exist. The excitation of the five-phase IM is assumed to be supplied by a five-phase current source inverter. In this case, each coil carries a quasi-rectangular current which consists of 72° pulses. The Fourier series of the current waveforms are given by eq. (2).

$$i_a(\theta) = \sum_{m=1}^{\infty} \left(\frac{4}{m\pi}\right) I_m \cos m\beta \sin(m\theta + \delta) \quad m = 1,3,5,\ldots \tag{2}$$

where, $\theta = \omega t$, $\beta = \frac{\pi}{10}$, δ is an arbitrary phase angle, and I_m is the average value of the DC link current. Since the current waveforms are symmetrical, it is clear that the even harmonics cannot exist.

The spatial magnetic motive force (MMF) pattern at any instant resulting from the coil currents is described by the sum of the instantaneous currents in all of the coils. The rotational movement of the MMF pattern with time is decided by the time variation of these currents; i.e. the current waveforms. Let F be the total MMFs produced by coils a, b, c, d, and e.

TABLE I
RELATIONSHIP BETWEEN FIELD SPACE HARMONICS AND CURRENT TIME HARMONICS FOR A FIVE-PHASE IM HAS A CONCENTRATED WINDING

		Space Harmonics							
		1	3	5	7	9	11	13	15
Time Harmonics	1	F 1.156	-	-	-	B .128	F .105∠180°	-	-
	3	-	F .079∠180°	-	B .034∠180°	-	-	F .0183	-
	5	-	-	-	-	-	-	-	-
	7	-	B .034∠180°	-	F .0146	-	-	B .0078∠180°	-
	9	F .128∠180°	-	-	-	F .014∠180°	B .011	-	-
	11	F .105∠180°	-	-	-	B .011∠180°	F .009	-	-
	13	-	F .183	-	B .0078	-	-	F .0042∠180°	-
	15	-	-	-	-	-	-	-	

Then:

$$F = N_a i_a + N_b i_b + N_c i_c + N_d i_d + N_e i_e = \sum_{n=1}^{\infty}\sum_{m=1}^{\infty}\left(\frac{1}{nm}\right)\left(\frac{4}{\pi}\right)^2 \frac{NI_m}{2}\cos\frac{m\pi}{10}((\cos(m\omega t - n\varphi)(\cos\frac{(m-n)2\pi}{5} + \cos\frac{(m-n)4\pi}{5} + \frac{1}{2}) + \cos(m\omega t + n\varphi)(\cos\frac{(m+n)2\pi}{5} + \cos\frac{(m+n)4\pi}{5} + \frac{1}{2})) \tag{3}$$

Accordingly, the relation between the field space harmonics and the current time harmonics for the concentrated five-phase winding is given numerically in Table I.

III. MATHEMATICAL MODEL

Based on the harmonic analysis in the previous discussion, the combined fundamental and third harmonic current, which is in shape similar to a rectangular waveform, can be simply considered as the input current of the five-phase IM instead of using the required rectangular current. Besides, the third harmonic does not interact with the fundamental components in both space and time. The MMFs and fluxes produced by the fundamental and the third harmonic rotate forward at the same synchronous speed. Therefore, the third harmonic acts as an equivalent fundamental component in a motor. The effects of the fundamental and the third harmonic can be directly imposed as two identical frequency components. Accordingly, the five-phase IM under the fundamental and third harmonic currents can be considered as two independent five-phase IM models as shown in Fig. 3.

The model of the five-phase IM in matrix form in the *abcde* reference frame can be described by the following equations.

The stator voltage equations:

$$V_{abcdes} = R_s I_{abcdes} + \frac{d\lambda_{abcdes}}{dt}. \tag{4}$$

The stator flux linkages equations:

$$\lambda_{abcdes} = L_s I_{abcdes} + L_{sr} I_{abcder}. \tag{5}$$

The rotor voltage equations:

$$V_{abcder} = R_r I_{abcder} + \frac{d\lambda_{abcder}}{dt}. \tag{6}$$

The rotor flux linkages:

$$\lambda_{abcder} = L'_{sr} I_{abcdes} + L_{rr} I_{abcder}. \tag{7}$$

And the torque equation:

$$T_e = \frac{P}{2} I^t_{abcdes} \frac{\partial L_s r}{\partial \theta_r} I_{abcder} \tag{8}$$

where, the stator voltage vector, the stator current vector, and the rotor current vector are:

$$V_{abcdes} = \begin{bmatrix} v_{as} & v_{bs} & v_{cs} & v_{ds} & v_{es} \end{bmatrix}^t;$$
$$V_{abcder} = \begin{bmatrix} v_{ar} & v_{br} & v_{cr} & v_{dr} & v_{er} \end{bmatrix}^t;$$
$$I_{abcdes} = \begin{bmatrix} i_{as} & i_{bs} & i_{cs} & i_{ds} & i_{es} \end{bmatrix}^t;$$
$$I_{abcder} = \begin{bmatrix} i_{ar} & i_{br} & i_{cr} & i_{dr} & i_{er} \end{bmatrix}^t;$$

where, t represents the transpose of a vector, P is the pole number, R_s is a five dimensional diagonal matrix consisting of the resistances of each stator phase, and R_r is a five dimensional diagonal matrix consisting of the resistances of each rotor phase.

The two space vectors which can equivalently express as, bs, cs, ds, and es-phase variables, not including the zero-sequence components, can be defined as follows:

$$F_{dqe1dqe3} = T_{13}(\theta) F_{abcdes} \tag{9}$$

Where,

$$F_{abcdes} = [\; F_{as} \quad F_{bs} \quad F_{cs} \quad F_{ds} \quad F_{es} \;]$$
$$[F_{dqe1dqe3n} = [\; F_{de1} \quad F_{qe1} \quad F_{de3} \quad F_{qe3} \;]$$
$$T_{13} = 2/5 \cdot$$
$$\begin{bmatrix} \cos\theta & \cos(\theta-\frac{2\pi}{5}) & \cos(\theta-\frac{4\pi}{5}) & \cos(\theta+\frac{4\pi}{5}) & \cos(\theta+\frac{2\pi}{5}) \\ \sin\theta & \sin(\theta-\frac{2\pi}{5}) & \sin(\theta-\frac{4\pi}{5}) & \sin(\theta+\frac{4\pi}{5}) & \sin(\theta+\frac{2\pi}{5}) \\ \cos 3\theta & \cos 3(\theta-\frac{2\pi}{5}) & \cos 3(\theta-\frac{4\pi}{5}) & \cos 3(\theta+\frac{4\pi}{5}) & \cos 3(\theta+\frac{2\pi}{5}) \\ \sin 3\theta & \sin 3(\theta-\frac{2\pi}{5}) & \sin 3(\theta-\frac{4\pi}{5}) & \sin 3(\theta+\frac{4\pi}{5}) & \sin 3(\theta+\frac{2\pi}{5}) \end{bmatrix}$$

The dynamic behavior of the five-phase IM is described by the following equations in the arbitrary rotating dqe_1dqe_3 reference frame.

$$V_{qe1} = R_s i_{qe1} + \omega\lambda_{de1} + \frac{d\lambda_{qe1}}{dt} \tag{10}$$

$$V_{de1} = R_s i_{de1} - \omega\lambda_{qe1} + \frac{d\lambda_{de1}}{dt} \tag{11}$$

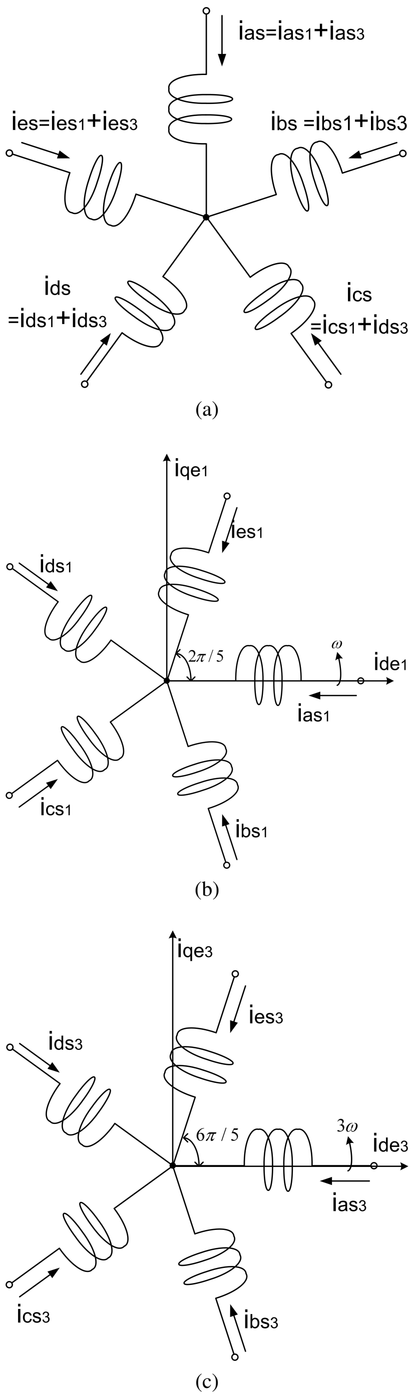

Fig. 3. Equivalent models of five-phase IM under the fundamental and third harmonic currents.

$$V_{qe3} = R_s i_{qe3} + 3\omega\lambda_{de3} + \frac{d\lambda_{qe3}}{dt} \tag{12}$$

$$V_{de3} = R_s i_{de3} - 3\omega\lambda_{qe3} + \frac{d\lambda_{de3}}{dt}. \tag{13}$$

IV. Proposed Motor Drive Algorithms

A. Direct Torque Control

The DTC method produces instantaneous torque control yielding a fast torque response and a very fast reversing operation. It is theoretically based on the principle of FOC AC motors. The main feature for DTC is that it does not need

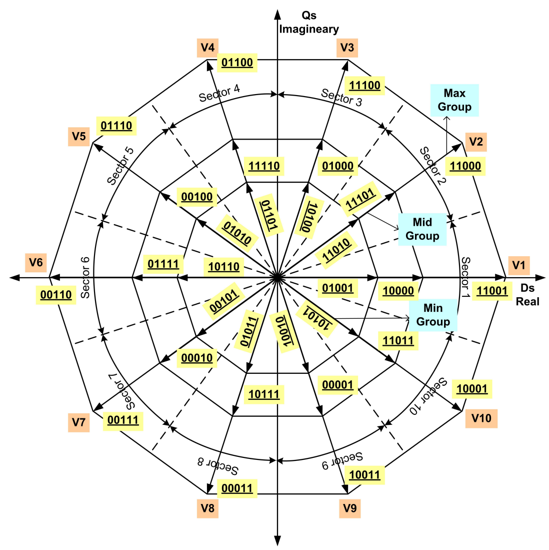

Fig. 4. Switching vectors for the five-phase IM drive.

a PWM controller for current control. In such a drive, the flux linkage and the electromagnetic torque are controlled directly and independently by the selection of optimum inverter switching vectors [14].

For the five-phase IM drives shown in Fig. 4, there are a total of thirty active switching vectors and two zero switching vectors. All these active switching vectors are divided into three groups which are the maximum, the medium and the minimum vectors. The only difference among the three groups is the length of the sides. The ratio of the amplitudes is given as follows:

$$\text{Min vector} = 2\cdot\cos(36) + 2\cos(72) - 1 = 1.236 \tag{14}$$

$$\text{Mid vector} = 2\cdot\cos(36) - 2\cos(72) + 1 = 2 \tag{15}$$

$$\text{Max vector} = 2\cdot\cos(36) + 2\cos(72) + 1 = 3.236. \tag{16}$$

Eq. (14)-(16) can be rewritten $1 : 1.618 : 1.6182^2$ from the minimum vector to the maximum vector, respectively.

Therefore, to minimize the switching loss it is better to use the maximum group. The other two groups are used when finer adjustments of the stator flux and torque are needed [6].

To keep the advantages of DTC, the modified DTC, control q-axis stator current and the d-axis stator current using an optimal voltage switching look-up table, is proposed. Fig. 5 shows the schematic of the proposed DTC for the five-phase IM drive, which uses a transformed stator current to control the torque and the stator flux. In the torque component current producing the dq-axis plane, the inverse park transformation are used same as in FOC.

The synchronous rotating angle θ in axis-transformation is considered as the sum of three angles.

$$\theta = \theta_r + \theta_{slip} + \alpha \tag{17}$$

where, θ_r, θ_{slip}, and α represent the rotor position, the slip angle, and the dynamic compensated angle, respectively.

$$\alpha = \arctan(i_{qs1}/i_{ds1}). \tag{18}$$

As described previously, the goal of the proposed DTC of a five-phase IM is to maintain the d-axis current and the

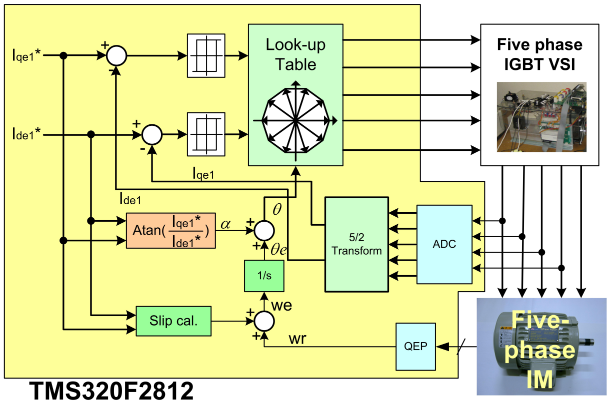

Fig. 5. DTC for five-phase IM drive.

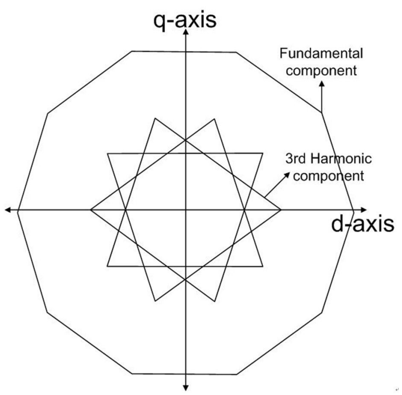

(a) Vector locus in dq1-dq3.

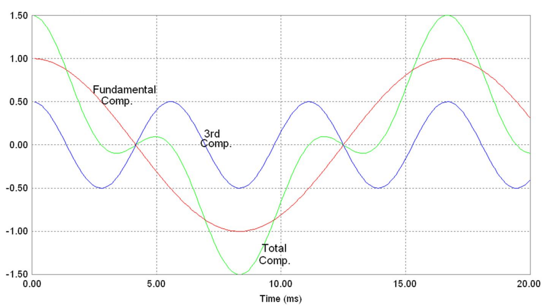

(b) Current waveform.

Fig. 6. Five phase space vector locus in dq1 and dq3 frame, and corresponding current waveform.

q-axis current within the limit of the hysteresis bands by proper selection of the stator space voltage vectors during each sampling period. The maximum group of voltage vectors is selected according to the errors of the d-q axis current. Table II summaries the combined effect of each voltage vector both on the d-axis current and the q-axis current.

The proper voltage vector should be applied based on the d-axis stator current and the q-axis current errors with respect to their reference values. For example, suppose that the stator flux linkage vector is in the first sector in Fig. 4 and only the maximum group is considered. Now if the d-axis current for flux component has to be increased (FI) and the q-axis current for torque component has to be positive (TP), then the switching voltage vector is selected as V2.

On the other hand, if the d-axis current has to be increased (FI) and the q-axis current need to be negative (TN), then the vector V10 has to be selected. The voltage vectors located on the other two decagons have similar effects with respect to the larger decagon.

Based on the above, the increased number of space voltage vectors allows for the generation of a more elaborate switching vector table in which the selection of the voltage vectors is made according to real-time variations of the flux-component current and the torque-component current. The optimum voltage vector can be given as below:

$$\begin{aligned} &dI_{de1}=1 \ \& \ dI_{qe1}=1 \text{ then } V_{epi}=V(sector+1)\\ &dI_{de1}=1 \ \& \ dI_{qe1}=-1 \text{ then } V_{epi}=V(sector-1)\\ &dI_{de1}=0 \ \& \ dI_{qe1}=1 \text{ then } V_{epi}=V(sector+3)\\ &dI_{de1}=0 \ \& \ dI_{qe1}=-1 \text{ then } V_{epi}=V(sector-1). \end{aligned} \tag{19}$$

Above mention in Table I, if the equivalent circuits of a five-phase IM have a space harmonic component, it will deform current waveform [15]. It will now be determined what happens if the 3rd time harmonic plus fundamental components are used to produce the reference with a circular locus in the $d_{e1}-q_{e1}$ plane. In Fig. 6(a), the corresponding space vector locus is plotted in the d_qe1 and d_qe3 frames. The locus shape of the d_qe3 frame indicates the 3rd harmonics current. In the time domain, the 3rd voltage harmonics will superpose onto the fundamental component in the $d_{e1}-q_{e1}$ frame and the phase current will thus be deformed. Since the fundamental voltage and 3rd harmonic voltages apply to different equivalent circuits, the harmonic current will have a different phase shift. Also, the small impedance without back EMF terms in the $d_{e3}-q_{e3}$ frame circuit induces a large magnitude harmonic current which is almost comparable to that of the fundamental, as can be seen in Fig. 6(b). Therefore, the elimination of this harmonics component from the voltage signal is necessary. However, it is almost impossible to reduce and inject the 3rd harmonic component using the DTC method.

B. Rotor Field Oriented Control [RFOC]

Based on the RFOC model developed for the five-phase IM with the fundamental and third harmonics, the block diagram of the RFOC is schematically depicted in Fig. 7. The coefficient 0.15 in Fig. 7 is associated with the relative value of the third harmonic stator current dqe3 references with respect to the dqe1 current references. In order to supply a trapezoidal stator phase current, the 3rd harmonic current component is added and its value is set, for the following experimentally obtained results, to 15% [16].

The third harmonic torque and the flux component of the stator currents (I^*_{qe3} and I^*_{de3}) are given by 15% of I^*_{qe1} and I^*_{de1}. Integrating the transformation matrix $T_{13}(\theta)$ and the reference currents I^*_{qe1}, I^*_{qe3},I^*_{de1} and I^*_{de3} the stator reference currents i^*_{as}, i^*_{bs}, i^*_{cs}, i^*_{ds} and i^*_{es} can be obtained.

The current loop, which uses fixed frequency hysteresis current controllers, makes the actual stator currents i_{as}, i_{bs},i_{cs}, i_{ds} and $i$es and tracks both the commanded fundamental and third harmonic currents. To keep the same effective currents, the fundamental components and the third harmonic components of the stator reference currents i^*_{as}, i^*_{bs}, i^*_{cs}, i^*_{ds} and i^*_{es} are

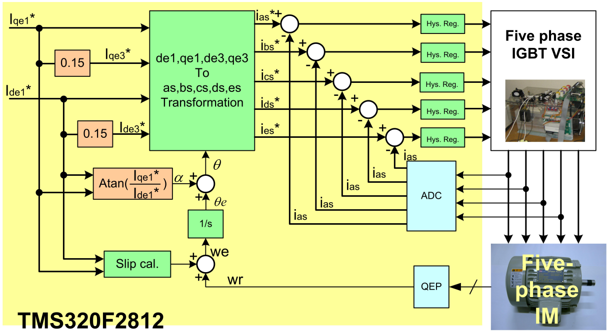

Fig. 7. Block diagram of RFOC of five-phase IM drive with the fundamental and third harmonic currents.

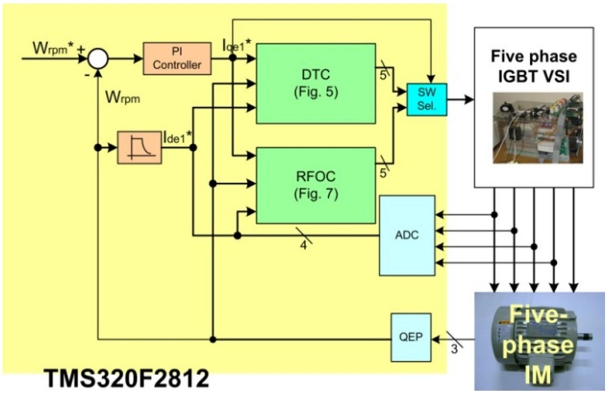

Fig. 8. Block diagram of the proposed five-phase IM drive excluding effects of 3rd current harmonics component.

properly adjusted. Angle (eq.18) is the dynamic compensating angle.

Through dynamic adjustment of the fundamental currents and the third harmonic of the fundamental current waveform, the desired FOC, the nearly rectangular current waveform and the flux distribution can be achieved [17].

C. The Proposed Control Scheme

In order to exclude the effect of the 3rd current harmonic component during the steady state and to keep the advantages of traditional DTC during the dynamic state, the modified DTC of a five-phase IM drive is shown in Fig. 8.

To keep the benefits of DTC during the transient state, the calculation of the torque and flux component current is used with the traditional park transformation. The calculation of the flux error and torque error is done through two hysteresis regulators and a look-up table. Detailed strategies on how to decide the desired voltage vector are explained in section A. In order to reduce the torque and current ripple during the steady state, the scheme of using the inverse park transformation and a five-hysteresis regulator to derive the reference voltage is adopted in this paper, and its principle is illustrated in Fig. 7. Mode selection of the steady state and the transient state uses the reference value of the torque component current (I^*_{qe1}). If the absolute value of I^*_{qe1} is over 0.3[PU], then DTC is selected and if the absolute value of I^*_{qe1} is below 0.3[PU], then RFOC is selected.

As a result, the proposed algorithm does not require a PI controller for current regulation and it can control the 3rd harmonic component, which means that this algorithm can exclude effect of the 3rd harmonic current that causes current distortion and result in a much lower torque ripple.

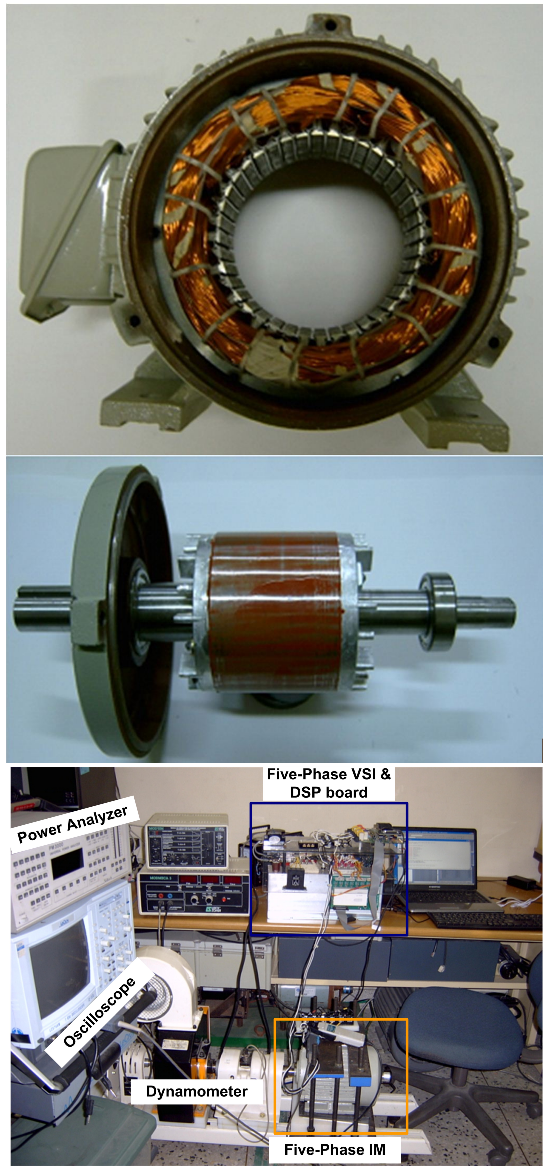

Fig. 9. Five-phase IM and experimental setup.

V. Experimental Results

The proposed five-phase IM has been fabricated in the laboratory. Fig. 9 shows the five-phase stator, the rotor and the experimental setup. A five-leg IGBT-based inverter has also been fabricated in the laboratory. A TMS320F2812 DSP is used to implement the digital control. The motor parameters are listed in Table III. To verify the theoretical analysis and the algorithms, several experiments are performed.

Fig. 10 shows the steady state characteristics using the look-up table DTC at 900[rpm] as shown in Fig.5. As can be seen, there is a remarkable current distortion because of the 3rd current harmonic component in Fig. 10(a). Fig. 10(b) and (c) present waveforms of torque component current (I_{qe1}) and the flux component current (I_{de1}). As can be seen from the figure I^*_{qe1} is set to 0.79[A] and I^*_{de1} is set to 0.66[A]. Fig 10(d) represents the FFT results for the phase current. As can be seen

TABLE II
OPTIMUM ACTIVE VOLTAGE VECTOR LOOK-UP TABLE

DI_{de1}	DI_{qe1}	Sector1	Sector2	Sector3	Sector4	Sector5	Sector6	Sector7	Sector8	Sector9	Sector10
1	1	V2	V3	V4	V5	V6	V7	V8	V9	V10	V1
1	-1	V10	V1	V2	V3	V4	V5	V6	V7	V8	V9
0	1	V4	V5	V6	V7	V8	V9	V10	V1	V2	V3
0	-1	V8	V9	V10	V1	V2	V3	V4	V5	V6	V7

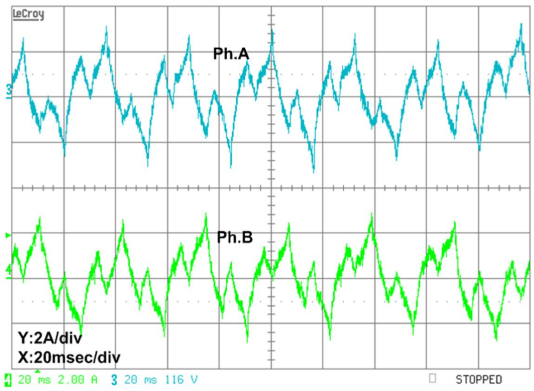

(a) Phase current waveform.

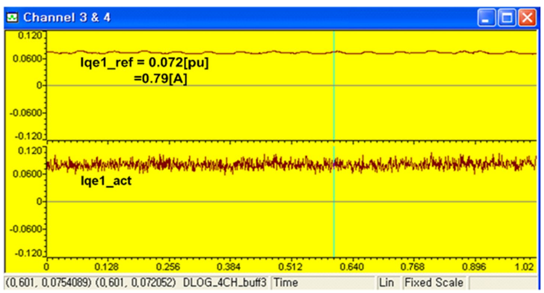

(b) Torque component current(Iqe1) waveform.

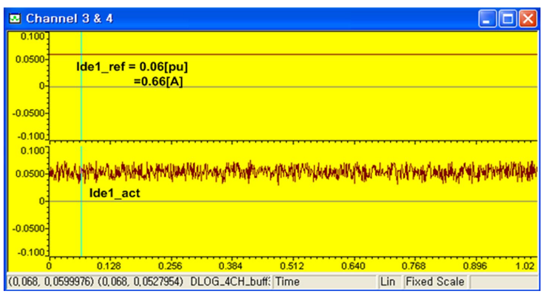

(c) Flux component current(Ide1) waveform.

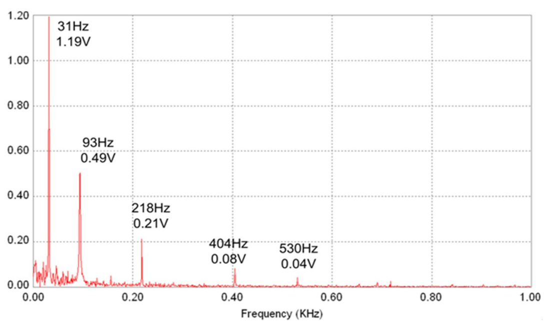

(d) FFT result of phase current.

Fig. 10. Experimental results of DTC.

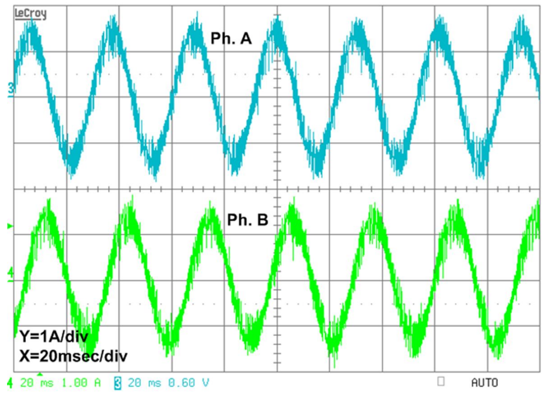

(a) Phase current waveform.

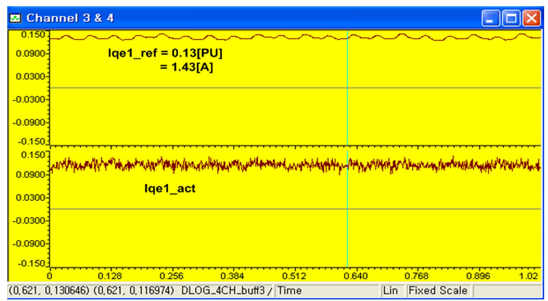

(b) Torque component current(Iqe1) waveform.

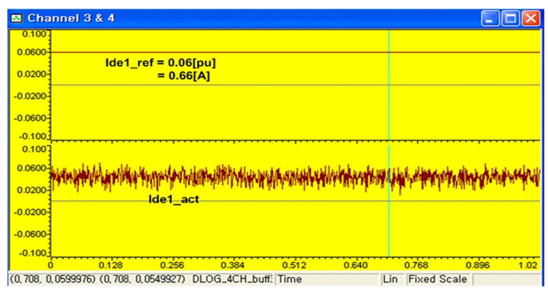

(c) Flux component current(Ide1) waveform.

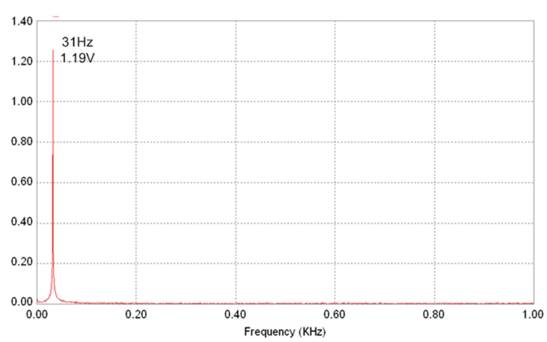

(d) FFT result of phase current.

Fig. 11. Experimental results of RFOC with k=0.0.

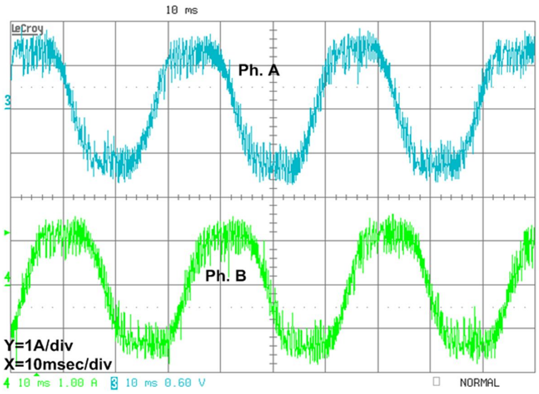

(a) Phase current waveform.

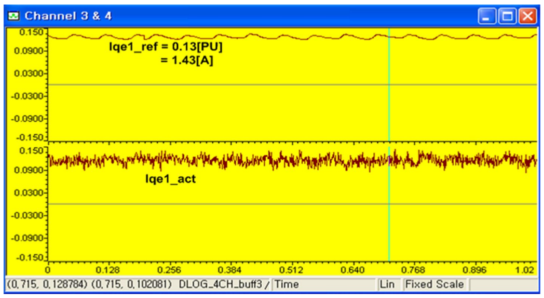

(b) Torque component current(Iqe1) waveform.

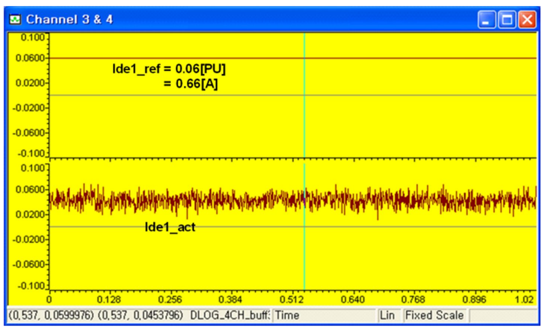

(c) Flux component current(Ide1) waveform.

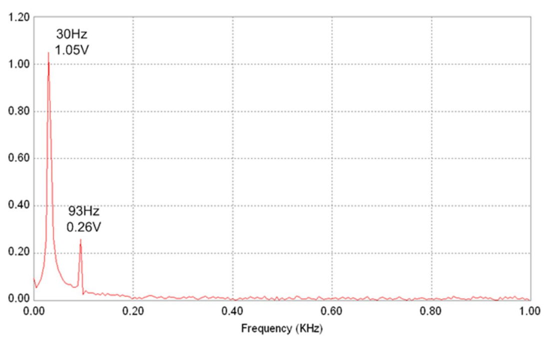

(d) FFT result of phase current.

Fig. 12. Experimental results of RFOC with k=0.15.

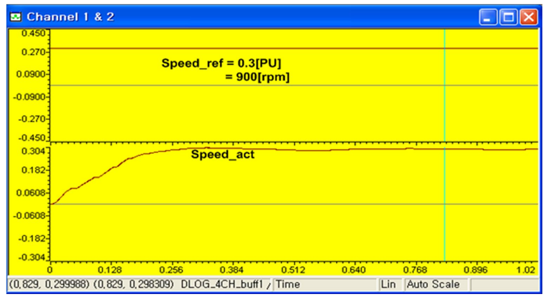

(a) Phase current waveform.

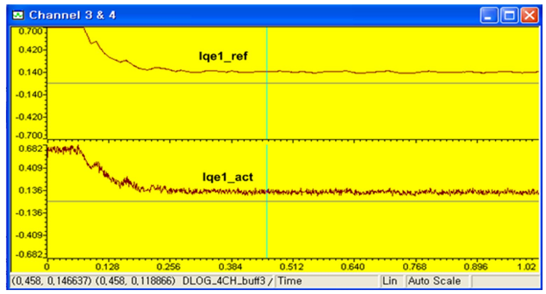

(b) Torque component current(Iqe1) waveform.

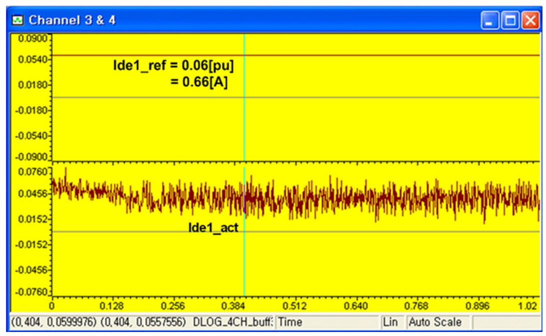

(c) Flux component current(Ide1) waveform.

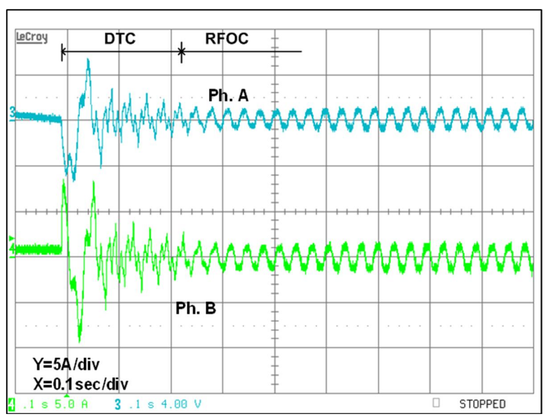

(d) FFT result of phase current.

Fig. 13. Experimental results of proposed scheme.

TABLE III
PARAMETERS OF THE FIVE-PHASE IM

Item	Parameter
Rated Power	1.5hp
Phase voltage	220V
Rated current	5.0A
Poles No.	4
Rated frequency	60Hz
Rs[ohm]	6.30
Rr[ohm]	4.08
Ls[mH]	0.6517
Lr[mH]	0.6517
Lm[mH]	0.6236

from the figure the phase current has huge current harmonic components, which are 3rd, 7th, etc. Therefore the presence of the 3rd current harmonic component should be eliminated to get good steady state characteristics.

Fig. 11 shows the steady state characteristics using the RFOC ($k = 0.0$) at 900[rpm] as shown in Fig. 7. Where k is a ratio of the 3rd harmonic component in terms of the fundamental component. As can be seen, there are no 3rd current harmonic components in Fig. 11(a). Presented in Fig. 11(b) and (c) are the waveforms of the torque component current (Iqe1) and the flux component current (Ide1) in the synchronously rotating reference frame. As can be seen from the figure I_{qe1}^* is set to 1.43[A] and I_{de1}^* is set to 0.66[A]. Fig 11(d) represents the FFT results of the phase current. As can be seen from the figure the phase current has only the fundamental current component. Fig. 11 is in good agreement with Fig. 6 which has been explained in the theoretical study.

Fig. 12 shows the steady state characteristics using the RFOC ($k = 0.15$) at 900[rpm] as shown in Fig.7. As can be seen, there are 15% of the 3rd current harmonic component in Fig. 12(a). Presented in Fig. 12(b) and (c) are the waveforms of the torque component current (I_{qe1}^*) and the flux component current (I_{de1}^*) in the synchronously rotating reference frame. As can be seen from the figure I_{qe1}^* is set to 1.43[A] and I_{de1}^* is set to 0.66[A]. Fig 12(d) represents the FFT results of the phase current. As can be seen from the figure the phase current has only the fundamental and the 3rd current harmonic components.

Fig. 13 shows the dynamic characteristics from 0[rpm] to 900[rpm] as shown in Fig.8. Fig. 13(a) shows the speed characteristics. Fig. 13(b) and (c) presents the waveforms of the torque component current (I_{qe1}) and the flux component current (I_{de1}) in the synchronously rotating reference frame. Fig. 13(d) represents the waveforms of the phase A and B currents. As can be seen from the figure the proposed system provides a fast dynamic response and good steady state characteristics.

It can be observed from Fig. 10, 11 and 12 that the harmonics that appeared in the stator current waveforms in the conventional DTC are considerably reduced, and that they are similar to the sinusoidal and trapezoidal current waveforms achieved with the proposed control scheme.

It can be observed from Fig. 13 that speed of the permanent magnet synchronous motor drive tracks the reference values very well with excellent dynamic responses.

VI. CONCLUSION

Five-phase induction motors which have a rectangular back EMF using the look-up table DTC method suffer from two drawbacks. The first problem is the larger torque ripple when digital hysteresis implementation is used, which causes bearing currents that result in pitting and fluting of the motor bearings. The second is that it is almost impossible to inject the 3rd harmonic current component for maximizing the torque and the harmonic voltage causing the 3rd harmonic current can be introduced by the lookup table DTC method. To address these issues, the modified DTC based on RFOC is proposed. The inverse park transformation and a hysteresis controller are extended into a 5-phase system to exclude the 3rd harmonic current effect and to improve the steady-state performance. To maintain the advantages of conventional DTC and control torque, flux component control independently for five-phase IM, the modified DTC method using the d-axis and q-axis currents for finding the optimal voltage vector is suggested. Specifically, this paper introduced five-phase IM drive schemes to cancel out all of the possible 3rd harmonic frequency voltage harmonics. Detailed experimental results verify the effectiveness of the proposed DTC method in steady-state performance.

REFERENCES

[1] N. Bianchi, S. Bolognani, and M. D. Pre, “Strategies for the fault-tolerant current control of a five-phase permanent-magnet motor,” *IEEE Trans. on Ind. Appl.*, Vol. 43, No. 4, pp. 960 – 970, Jul./Aug. 2007.

[2] C. C. Chan, J. Z. Jiang, G. H. Chen, and X. Y. Wang, “A novel high power density permanent magnet variable-speed motor,” *IEEE Trans. Energy Convers.*, Vol. 8, No. 2, pp. 297-303, Jun. 1993.

[3] E. Levi, M. Jones, S. N. Vukosavic, and H. A. Toliyat, “Steady-state modeling of series-connected five-phase and six-phase two-motor drives,” *IEEE Trans. on Ind. Appl.*, Vol. 44, No. 5, Sep./Oct. 2008.

[4] S. Sadeghi and L. Parsa, “Design and dynamic simulation of five phase interior permanent magnet machine for series hybrid electric vehicles,” *2010 Green Technologies Conference*, pp. 1-6, 2010.

[5] L. Parsa and H. M. Toliyat, “Five-phase permanent-magnet motor drives,” *IEEE Trans. Ind. Appl.*, Vol. 41, No. 1, pp. 30–37, Jan./Feb. 2005.

[6] H. Xu, H. A. Toliyat, and L. J. Petersen, “Five-phase induction motor drives with DSP-based control system,” *IEEE Trans. on Power Electron.*, Vol. 17, No. 4, pp. 524–533, Jul. 2002.

[7] Y. Kats, “Adjustable-speed drives with multiphase motors,” in Proc. *IEEE Int. Electric Machines Drives Conf.*, pp. TC2/4.1–TC2/4.3, May 1997.

[8] H. A. Toliyat, T. A. Lipo, and J. C. White, “Analysis of a concentrated winding induction machine for adjustable speed drive applications part 1(motor analysis),” *IEEE Trans. Energy Conv.,* Vol. 6, No. 4, pp. 679–683, Dec. 1991.

[9] H. A. Toliyat, T. A. Lipo, and J. C. White, “Analysis of a concentrated winding induction machine for adjustable speed drive applications part2 (motor design and performance),” *IEEE Trans. Energy Conv.*, Vol. 6, No. 4, pp. 684–692, Dec. 1991.

[10] K. N. Pavithran, R. Parimelalagan, and M. Krishnamurthy, “Studies on inverter-fed five-phase induction motor drive,” *IEEE Trans. Power Electron.*, Vol. 3, No. 3, pp. 224-235, Apr. 1988.

[11] H. A. Toliyat, “Analysis and simulation of five-phase variable speed induction motor drives under asymmetrical connections,” *IEEE Trans. Power Electronics*, Vol. 13, No. 4, pp. 748-756, Jul. 1998.

[12] H.-M. Ryu and S.-K. Sul, “Multiple d-q spaces concept for multi-phase AC motor drive,” *ICPE04*, pp. 670-674, 2004.

[13] A. Iqbal, “Dynamic performance of a vector-controlled five-phase synchronous reluctance motor drive: an experimental investigation,” *IET Electric Power Appl.*, Vol. 2, No. 5, pp. 298–305, Sep. 2008.

[14] M.-H. Kim, N.-H. Kim, and W.-S. Baik, "A high-performance sensorrless control system of reluctance synchronous motor with direct torque control by consideration of nonlinearly inductances," *Journal of Power Electronics*, Vol. 2, No.2, pp.146-153, Apr. 2002.
[15] Shuai Lu, K. Corzine, "Direct torque control of five-phase induction motor using space vector modulation with harmonics elimination and optimal switching sequence," *APEC '06*, 2006.
[16] H. A. Toliyat and T. A. Lipo, "Analysis of concentrated winding induction machines for adjustable speed drive applications-experimental results," *IEEE Trans. Energy Convers.*, Vol. 9, No. 4, pp. 695-700, Dec. 1994.
[17] M. J. Duran, F. Salas, and M. R. Arahal, "Bifurcation Analysis of Five-Phase Induction Motor Drives With Third Harmonic Injection," *IEEE Trans. on Ind. Electron.*, Vol. 55 , No. 5, pp. 2006–2014, May 2008.

ACKNOWLEDGMENT

This research was supported by Yeungnam College of Science & Technology Research grants in 2009.

Min-Huei Kim born in Kyengbuk Province, Republic of Korea in August, 1951. He received his B.S. and M.S. from Yeungnam University, Kyeungbuk, Korea, and his Ph.D. from the University of Chung-Ang, Seoul, Korea, all in Electrical Engineering, in 1974, 1980, and 1989, respectively. He worked in the Research and Development for Electric Motor Design Department of Shinil Industrial Company from 1977 to 1978, in Seoul, Korea. Since 1979, he has been with the Department of Automatic Electrical Engineering, Yeungnam College of Science and Technology, Daegu, Korea, where he is currently a Full Professor and a Director of the Power Application Technology Research Center (PATRC). From 1993 to 1995, he was a Visiting Research Professor in the Power Electronics Application Center (PEAC), University of Tennessee, Knoxville, USA. Prof. Kim received the Best Paper Competition Award and First Prize in IEEE IECON in 1996. Dr. Kim was listed in "Who's Who in the World 2001" on The Marquis Who's Who Publications Board, USA, and in "2000 Outstanding Intellectuals of the 21st Century 2003" at the International Biographical Centre Cambridge, UK. From 1998 to 2007, he held many positions in KIPE. He served as a Member of the Executive Board and worked in Technical Activities. He also held the positions of Treasurer, Vice President, and Auditor, for KIPE. He served as the Management and Organizer Committee Chair for ICPE 2004 and 2007. His research interests include the control of motor drives, power converters and the application of power electronics. He is a member of KIPE and JIEE, a life member of KIEE, and a senior member of IEEE.

Nam-Hun Kim was born in Kangwon Province, Republic of Korea in 1973. He received his B.S. in Control and Instrumentation Engineering from Samchuk National University in 1998, and his M.S. and the Ph.D. in Electrical Engineering from Yeungnam University, Kyeungbuk Province, Korea in 2000 and 2003, respectively. From 2004 to 2007, he was a Post Doctorate Researcher in the Department of Electrical and Computer Engineering, Texas A&M University, USA. He was a Full Time Instructor in the Department of Electrical Engineering, Chungju University, Korea, from 2008 to 2009. He is currently a Principal Engineer at CnM Inc., Korea. He is currently engaged in research on motor control and design and the fault diagnosis of electrical machines. He is a member of KIPE and KIEE.

Won-Sik Baik was born in Daegu, Republic of Korea in October, 1970. He received his B.S. in Mathematics from Keimyung University, Daegu, Korea, in 1996, and his M.S. and Ph.D. in Electrical Engineering from Yeungnam University, Kyeungbuk Province, Korea, in 2001 and 2005, respectively. He was a Full Time Instructor in the Department of Automatic Electrical Engineering, Yeungnam College of Science and Technology, Korea, from 2008 to 2009. He is currently a Senior Researcher at LS Mechapion, Daegu, Korea. His research interests include the control of motor drives and power electronics. He is a member of KIPE and KIEE.